Preprint Title	A novel 3D flower-like Fe-photocatalyst with high degradative ability for water contaminant under visible light
Authors	Siwei Yang, Yuanfang Shen, Yixin Hong, Ankang Hu, Xuewei Tu, Yutong Chen, Jiefei Zhou, Yan Xu and Hui Zheng
Publication Date	28 Nov 2019
Article Type	Full Research Paper
Supporting Information File 1	Supporting Information.docx; 68.5 KB
ORCID® iDs	Siwei Yang - https://orcid.org/0000-0002-2659-1027; Hui Zheng - https://orcid.org/0000-0003-0785-6728

A novel 3D flower-like Fe-photocatalyst with high degradative ability for water contaminant under visible light

Siwei Yang, Yuanfang Shen, Yixin Hong, Ankang Hu, Xuewei Tu, Yutong Chen, Jiefei Zhou, Yan Xu and Hui Zheng*

Address

College of Material, Chemistry and Chemical Engineering, Hangzhou Normal University,

Hangzhou 311121, P.R. China

Email: huizheng@hznu.edu.cn

* Corresponding author

Abstract

A novel photocatalyst 2-amino-5-fluorobenzotrifluoride@Fe-based metal–organic framework (2A5F@Fe–MOF) was designed and synthesized, which exhibits excellent photocatalytic performance to degrade water contaminant rhodamine B (RhB) under visible light with 99.2% degradation rate after 2h. The photocatalyst was characterized by scanning electron microscopy (SEM), fourier transform infrared spectroscopy (FT-IR), X-ray diffraction (XRD) and X-ray photoelectron spectroscopy (XPS) as well as the analysis of morphological structure and chemical composition. Compared with pure Fe-MOF, the designed 2A5F@Fe-MOF photocatalyst appearance shows a transform from 2D to 3D, which maybe lead to the high photocatalytic activity toward RhB under visible light. The optimum conditions, such as ligand ratio, pH and concentration of RhB solution, were screened, also its degradation kinetic equations were built to give a typical reference for a large scale wastewater treatment.

Keywords

Photocatalyst; ligand; Fe-based MOF; rhodamine B; degradation

Introduction

Nowadays, dye wastewater pollution in textile industry has become a serious environmental problem, attracting more and more attention [1-3]. Rhodamine B (RhB) as a commercially used dye which has a certain representativeness in dye wastewater. According to the international agency for research on cancer (IARC), both inhalation and skin contact with RhB can cause acute and chronic toxic injuries [4].

In recent years, metal-organic frameworks (MOFs) have attracted extensive attention in sensor, catalysis, gas storage and photochemical devices due to its high specific surface area and adjustable porous size. Also, due to the different potential electric charge transfer transitions between ligands and metals, MOFs as a photocatalyst has attracted continuous attention [5-7].A large number of research results reflect the growing interest in the application of MOF based composites and their derivatives in dye degradation [8-11]. Many methods for obtaining MOFs-related nanomaterials with high catalytic activity were studied. These approaches include the direct usage of MOFs exhibiting intrinsic photocatalytic activity (Ti-MOF, Fe-MOF, or Cu-MOF) [12-15] and the introduction of other components into MOFs to enhance dye adsorption or photocatalytic activity [16-18].

Due to iron's low toxicity and high biocompatibility, iron-based MOFs are particularly desirable for environmental applications [19-23]. Furthermore, iron oxides are rich in sources, cheap and have been widely used in magnetic fluid, magnetic recording, multifunctional catalysts and biomedicine. It is easily activated and absorbed by visible light for its narrow bandgap, therefore it can also be used as a visible light photocatalyst matrix. Zhang [24] used an ultrasonic assisted self-assembly preparation method to synthesize α-Fe_2O_3@g-C_3N_4 photocatalyst. The α-Fe_2O_3@g-C_3N_4 photocatalyst had a stronger optical absorption in the visible light region than pure graphitic carbon nitride (g-C_3N_4). He [25] synthesized the iron-based NH_2-MIL-88B (Fe) metal organic framework by a facile and rapid microwave heating

method. The photodegradation results show that NH_2-MIL-88B(Fe) can be used as a peroxidase-like catalyst for Fenton-like degradation of methylene blue (MB) in water. As we all known, visible light is the best source in nature to degrade contaminants, it is an interesting challenge to design the specific catalyst to absorb visible light. While, with the larger bandgap, the catalyst become more difficult to be excited by visible light. Therefore, designing novel ligands supported on such oxides to decrease the bandgap of catalyst, which can increase the possibility of photocatalyst excited by visible light, is a challenging task.

For our continuous interest and previous experience about developing novel photocatalyst to degrade water contaminants [26], we try to employ a simple ligand containing strong electron-withdrawing group which could be doped on Fe-MOF to decrease the band gap of photocatalyst so as to utilize solar energy directly. The commercial intermediate 2-amino-5-fluorobenzotrifluoride was selected to perform and verify this hypothesis. Fortunately, it works well when treating the pollutant RhB under visible light. It is worth mentioning that the interface of this novel ligand-doped photocatalyst has obvious appearance changes from 2D to 3D compared to the pure Fe-MOF, which maybe lead to the high photocatalytic activity toward RhB under visible light.

Experimental

2A5F@Fe-MOF was prepared according to the synthetic process below. Sodium dodecyl sulfate (5mmol, 1.45g) was added into the mixed iron (III) trichloride (40mmol, 6.48g) and the iron (II) dichloride tetrahydrate (20mmol, 3.98g) in deionized water (50mL) with stirring. After stirred for 1h, the solution of 2-amino-5-fluorobenzotrifluoride (10mmol, 1.79g) [n(Ligand): n(MOF)=1:2] in 50% (v/v) ethanol aqueous solution (20mL) was added. The solution was stirred overnight. The obtained brown precipitate was centrifuged, washed with deionized water, and dried at 80°C for 6h, successively. As a result, 50%2A5F@Fe-MOF was obtained. Fe-MOF, 25%2A5F@Fe-MOF and 100%2A5F@Fe-MOF were synthesized in the

same manner, only with the different amount addition of 2-amino-5-fluorobenzotrifluoride as the organic ligand.

The chemical composition of 2A5F@Fe-MOF composite was characterized by Fourier transform infrared (FT-IR, Bruker 55FT-IR). The scanning electron microscopy (SEM) measurements (S-4800, HITACHI) with an accelerating voltage of 15 kV was utilized to analyse morphologies structure. X-ray diffraction (XRD) patterns were recorded by X-ray diffraction (XRD, Bruker D8 Advance) patterns were recorded using Cu Kα radiation (40 kV and 40 mA) and scanning rate of $2° \cdot min^{-1}$. Chemical state of iron was analysed X-ray photoelectron spectroscopy (XPS, Thermo ESCALAB 250XI). UV–Vis diffuses reflectance spectra was also obtained (DRS, Hitachi U-3900H).

The photocatalytic activities of photocatalysts were evaluated by the photo-degradation of rhodamine B (RhB) under visible light. In the typical experiment process, 0.1mg of the photocatalyst was added into the 20mL rhodamine B solution (20mg/L). Prior to irradiation, the suspensions were magnetically stirred for 30 minutes in the dark at room temperature to reach the adsorption-desorption equilibrium. The solutions were then irradiated with the solar simulator (Newport 94023A, USA). At specific time intervals of 20 minutes, 1mL of the solution was withdrawn from the system and centrifuged (4000rpm, 5min) to remove the photocatalyst particles. The degradation rate was monitored by UV-Vis spectrometer (Beckman Coulter DU730) at room temperature. The degradation efficiency (DE) was calculated using the equation: $DE=[(A_0-A_t)/A_0] \times 100\%$. Where A_0 is the initial absorbance of solution and A_t is the absorbance of solution at a specific time.

Results and Discussion

The morphology and microstructure of the photocatalyst were studied using SEM. As shown in Figure 1a, it can be easily observed that the pure Fe-MOF had a smooth layer macrostructure. And its microstructure still remained a 2D layer (Figure 1b). After the ligand

doping, this photocatalyst appearance turned to a 3D structure (Figure 1c), whose microscopic spectrum showed a flower-like structure (Figure 1d). This flower-like structure greatly increases the specific surface area of the photocatalyst, which is the photocatalytic reaction site, thereby enhancing the photocatalytic properties of Fe-MOF.
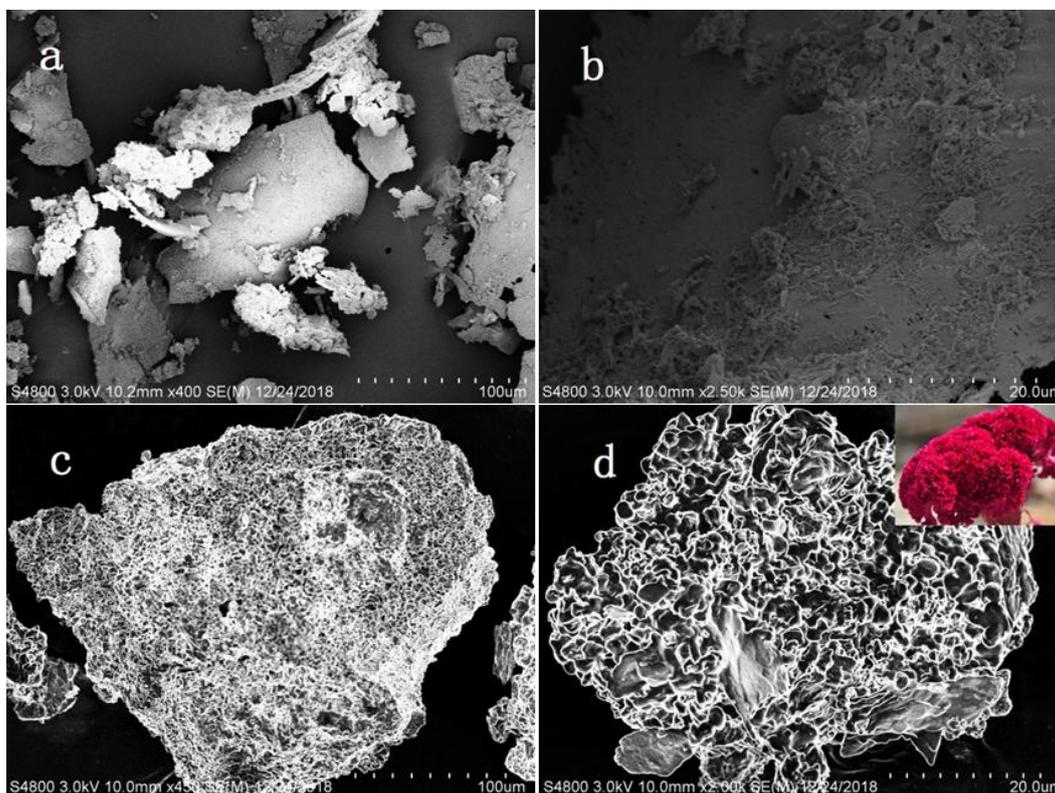
Figure 1: SEM images of Fe-MOF (a, b) and 50%2A5F@Fe-MOF (c, d)

As shown in Figure 2, five peaks are observed in the XRD pattern of Fe-MOF. 26.9°, 35.42°, 43.3°, 56.1°and 61.3° (2Theta) are belong to the (220), (311), (400), (511) and (440) plane diffractions of Fe_3O_4 (JCPDS card No.19-0629), respectively. The XRD pattern of the 50%2A5F@Fe-MOF shows the peak strength was decreased and part of the peak were disappeared compare with Fe-MOF. These findings imply that the main structure of Fe-MOF remains but a small part of the surface is covered by the ligand after doping, which may lead to a large increase in photocatalytic activity.
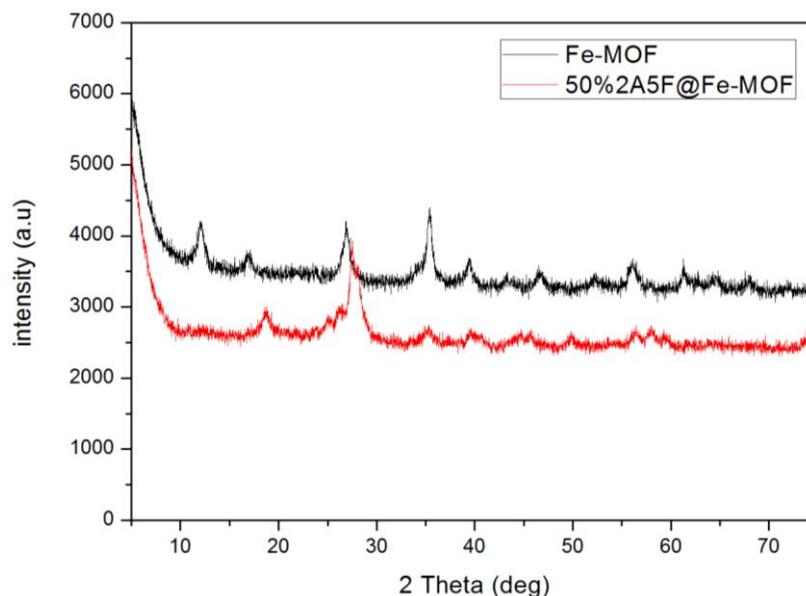
Figure 2: XRD spectra of Fe-MOF and 50%2A5F@Fe-MOF

XPS spectra of Fe 2p was carried out to determine the Fe state in Fe-MOF. The results were shown in Figure 3 where 'sat.' represents the satellite peak in the XPS spectrum. All the elements were corrected by C 1s at 284.8 eV. The percentage of Fe^{3+} and Fe^{2+} were calculated to be 41.9% and 58.1%, respectively, using curve-fitting [27]. The decrease of Fe^{3+} is mainly attributed to the washing process.
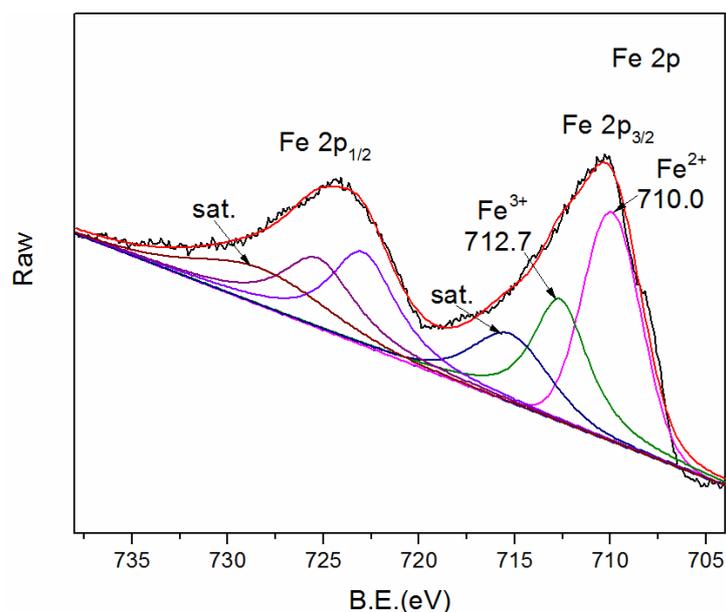
Figure 3: Fe 2p XPS of Fe-MOF

Uv-vis absorption spectra were shown in Figure 4. As we can see in Figure 4a, after the ligand 2A5F was doped, the visible light absorption capacity of Fe-MOF was greatly enhanced at

visible region. The direct bandgap energies (Eg) of Fe-MOF and 50%2A5F@Fe-MOF were estimated to be 2.08 and 1.91eV respectively, using formula [28,29]:

$$\alpha h\nu = A(h\nu - Eg)^{1/2}$$

The decline of Eg after ligand doping can effectively enhance the visible light excitation ability of photocatalyst, which was confirmed by following degradation experiment that degradation rate jumped from almost zero to 99.2%.
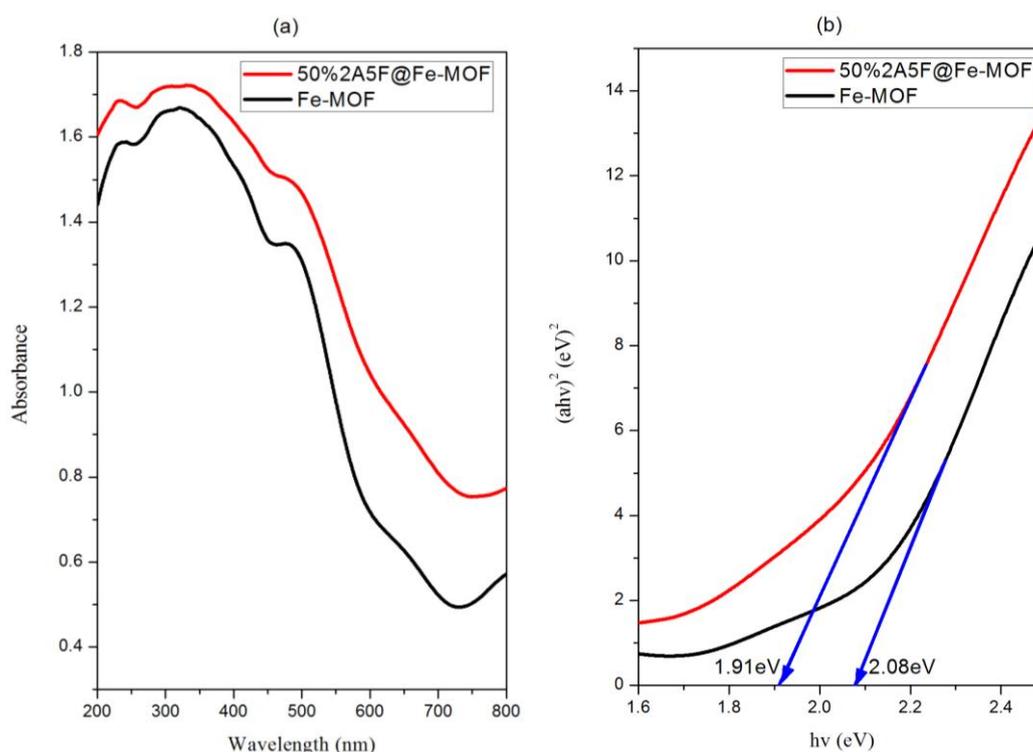
Figure 4: (a) The UV−Vis diffuses reflectance spectra of Fe-MOF

and 50%2A5F@Fe-MOF, (b) the band gap energies

FT-IR spectroscopy was carried out to confirm the existence of ligand on the as-prepared catalyst. The results indicate that the ligand is successfully loaded on the photocatalyst particles. The strong band at 1380 cm^{-1}, assigned to C-F stretching. And the bands at 1600 and 1480 cm^{-1}, assigned to skeleton vibration of benzene. The peak at 3450 cm^{-1} is assigned to N-H bond. The absence of other two peaks near 2950 and 2850 cm^{-1} corresponds to C-H stretching vibrations of benzene.

Optimization of Photocatalytic conditions

Ligand ratio of photocatalyst

Figure 5a shows the photocatalytic performance of 2A5F@Fe-MOF composites towards 20mg/L RhB solution under visible light irradiation, respectively. It is observed that the photocatalytic efficiency of as-prepared Fe-MOF is nearly close to zero. Moreover, with the presence of 2A5F@Fe-MOF, the degradation efficiency is increased. 50%2A5F@Fe-MOF has the highest degradation rate which reached a maximum value of 99.2% after 2h treatment. As shown in figure 5b, the first-order kinetics rate constant was calculated using the following equation [30]:

$$k = -\ln(A_0/A_t)$$

where "k" is the degradation rate constant (min^{-1}). The degradation rate constants were $1.298*10^{-4}$ min^{-1}, $1.038*10^{-2}$ min^{-1}, $1.625*10^{-2}$ min^{-1} and $1.143*10^{-2}$ min^{-1} for Fe-MOF, 25%2A5F@Fe-MOF, 50%2A5F@Fe-MOF and 100%2A5F@Fe-MOF, respectively. 50%2A5F@Fe-MOF showed the highest degradation rate constant, which is 125 times higher than Fe-MOF (figure 5c). The recycle experiment also showed that 50%2A5F@Fe-MOF has excellent stability, the degradation efficiency of 20mg/L rhodamine solution remains at 92% after 5 runs (figure 5d).
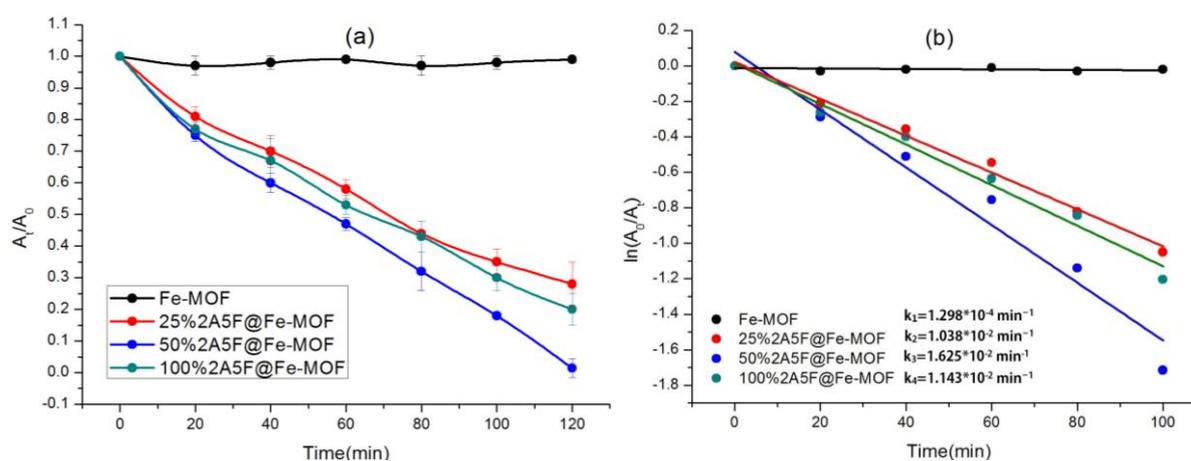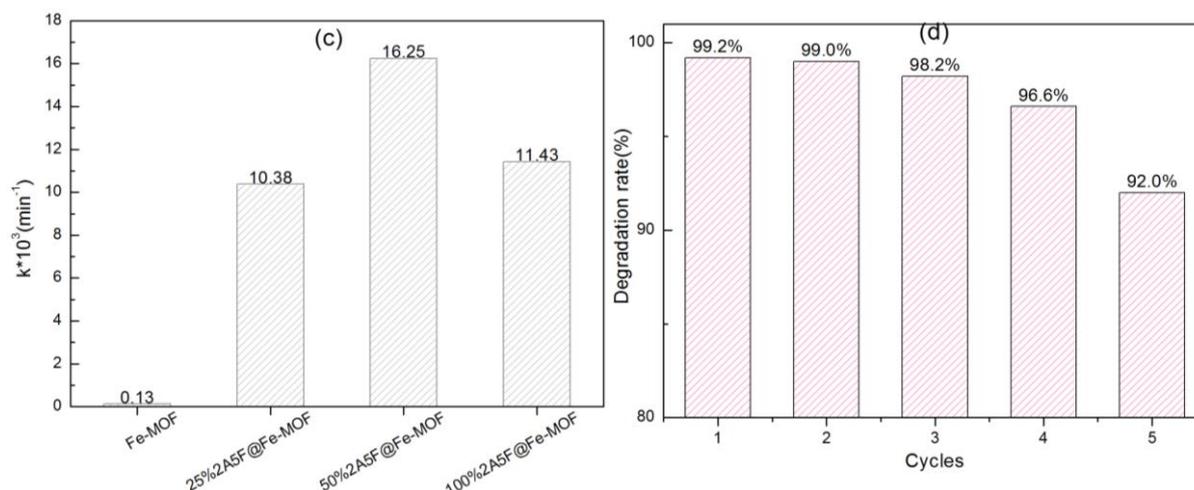
Figure 5: (a) effect of ligand ratio, (b) kinetic curves of the photocatalysts,

(c) rate constant of the photocatalysts, (d) recycling studies of 50%2A5F@Fe-MOF

pH of RhB solution

The effect of pH on photocatalytic activity was determined by degrading 20mg/L RhB solution at seven pH values: 1.0, 3.0, 5.0, 7.0, 9.0, 11.0 and 13.0 (Figure 6). The degradation rate of RhB was 99.2% after 2 h treatment without pH adjustment (pH=7.0). The degradation rates were 0.8%, 1%, 3.1%, 80.1%, 54.5% and 37% when the initial pH values were 13.0, 11.0, 9.0, 5.0, 3.0 and 1.0 after 2h treatment, respectively. The degradation rate was lower under acidic solution and alkaline solution, while the degradation rate of neutral solution was the highest.
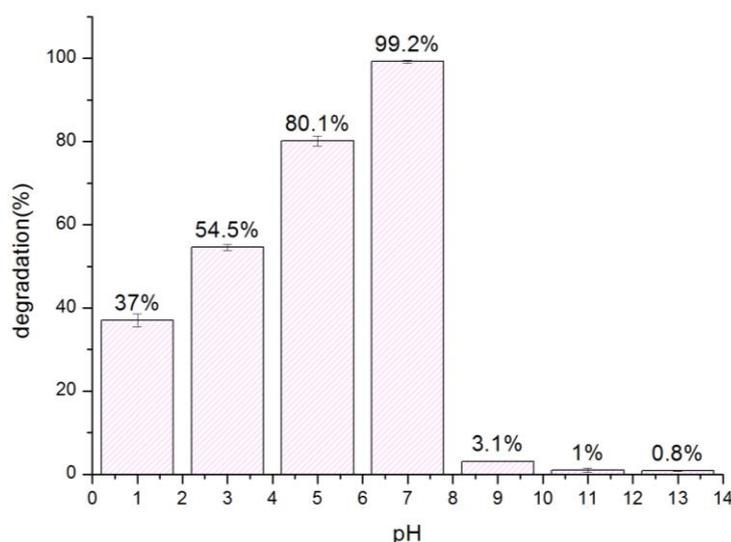
Figure 6: Photocatalytic degradation of RhB at different pH

Concentration of RhB solution

Figure 7 shows the catalyst has a high degradation rate for RhB with a concentration of less than 40 mg/L. The degradation rate decreased a lot when the concentration comes to 80 mg/L. This may due to the concentrations of photocatalyst were limited, which was not enough for the degradation with higher concentration.
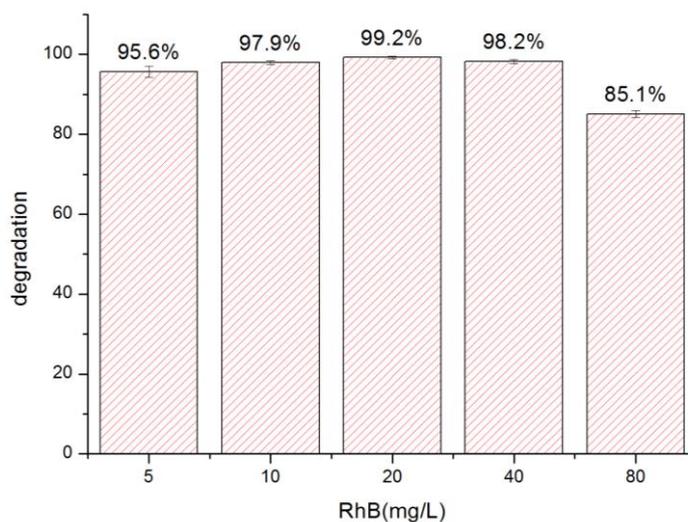
Figure 7: Photocatalytic degradation of RhB at different concentrations

Proposed degradation mechanism

Figure 8 shows the proposed mechanism for the photogenerated charges transfer process in the 2A5F@Fe-MOF photocatalyst. When the photocatalyst is irradiated, photogenerated electrons excited from the Fe-MOF are transferred along the hydrogen bonds to the surface ligand molecules, where the oxygen(O_2) can be turned to superoxide radical($\cdot O_2^-$) ,which reducing the probability of recombination with photogenerated holes. Resulting the photogenerated holes and superoxide radicals can further degrade rhodamine in the solution.
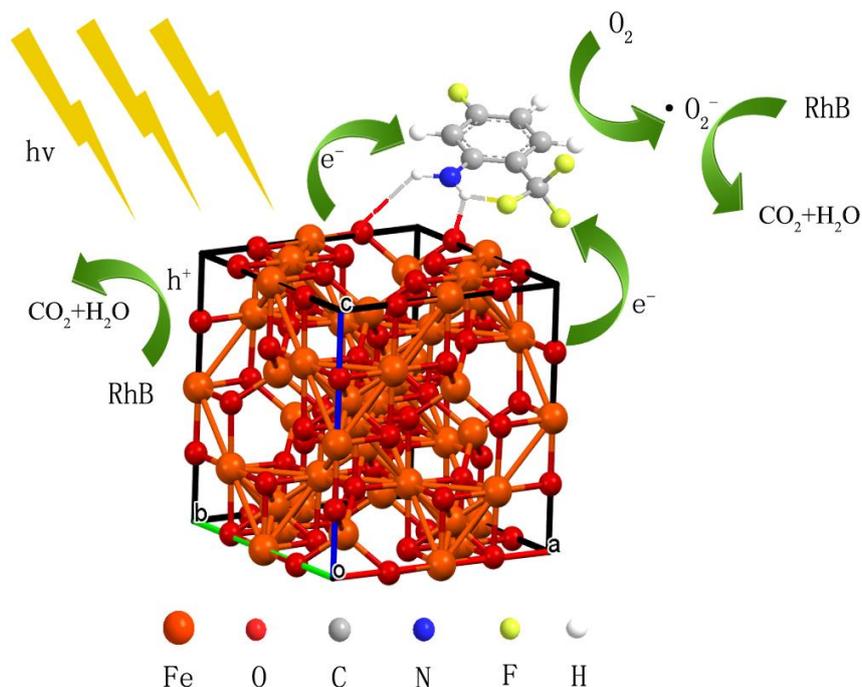
Figure 8: Schematic diagram of the transfer of photogenerated charges under irradiation

Conclusion

In this work, a novel photocatalyst 2A5F@Fe-MOF were developed for the water contaminant degradation. The morphological structure and photocatalytic performance of Fe–MOF shows significant changes after the ligand doping. The morphology of photocatalyst transformed from 2D layer to 3D flower-like. And the optimum conditions for RhB degradation were carried out for the large-scale degradation reference. The degradation rate reached 99.2% after 2h treatment when ligand ratio was 50%, pH was 7.0 and concentration of RhB was 20 mg/L. which means the ligand 2A5F remarkably improved the photocatalyst performance of Fe-MOF. Its impressive photocatalytic activity for the degradation of RhB proved that our initial assumption of designing ligand doped on Fe-MOF is feasible.

Acknowledgements

References

1. Ahmad, M.; Ahmed, E.; Zafar, F.; Khalid, N. R.; Niaz, N. A.; Hafeez, A.; Ikram, M.; Khan, M. A.; Hong, Z., Enhanced photocatalytic activity of Ce-doped ZnO nanopowders synthesized by combustion method. *Journal of Rare Earths* **2015,** *33* (3), 255-262.

2. Geng, X.; Chen, S.; Lv, X.; Jiang, W.; Wang, T., Synthesis of g-C_3N_4/Bi_5O_7I microspheres with enhanced photocatalytic activity under visible light. *Applied Surface Science* **2018,** *462*, 18-28.

3. Zhou, E.-H.; Li, B.-H.; Chen, W.-X.; Luo, Z.; Liu, J.; Singh, A.; Kumar, A.; Jin, J.-C., Photocatalytic degradation of organic dyes by a stable and biocompatible Zn(II) MOF having ferulic acid: Experimental findings and theoretical correlation. *Journal of Molecular Structure* **2017,** *1149*, 352-356.

4. Chen, Y.; Jin, X.; Guo, P., Preparation of Fe_3O_4 /$BiPO_4$ magnetic nanocomposite and its photocatalytic performance. *Journal of Molecular Structure* **2018,** *1171*, 140-149.

5. Dhakshinamoorthy, A.; Alvaro, M.; Garcia, H., Commercial metal-organic frameworks as heterogeneous catalysts. *Chemical communications* **2012,** *48* (92), 11275-88.

6. Laurier, K. G.; Fron, E.; Atienzar, P.; Kennes, K.; Garcia, H.; Van der Auweraer, M.; De Vos, D. E.; Hofkens, J.; Roeffaers, M. B., Delayed electron-hole pair recombination in iron(III)-oxo metal-organic frameworks. *Physical chemistry chemical physics : PCCP* **2014,** *16* (11), 5044-7.

7. Liu, J.; Chen, L.; Cui, H.; Zhang, J.; Zhang, L.; Su, C. Y., Applications of metal-organic frameworks in heterogeneous supramolecular catalysis. *Chemical Society reviews* **2014,** *43* (16), 6011-61.

8. Ramasubbu, V.; Kumar, P. R.; Mothi, E. M.; Karuppasamy, K.; Kim, H.-S.; Maiyalagan, T.; Shajan, X. S., Highly interconnected porous TiO_2-Ni-MOF composite aerogel photoanodes for high power conversion efficiency in quasi-solid dye-sensitized solar cells. *Applied Surface Science* **2019,** *496*, 143646.

9. Yang, M.; Bai, Q., Flower-like hierarchical Ni-Zn MOF microspheres: Efficient adsorbents for dye removal. *Colloids and Surfaces A: Physicochemical and Engineering Aspects* **2019**, 582, 123795.

10. Akbarzadeh, E.; Soheili, H. Z.; Hosseinifard, M.; Gholami, M. R., Preparation and characterization of novel Ag_3VO_4/Cu-MOF/rGO heterojunction for photocatalytic degradation of organic pollutants. *Materials Research Bulletin* **2020,** *121*, 110621.

11. Aleksandrzak, M.; Baranowska, D.; Kedzierski, T.; Sielicki, K.; Zhang, S.; Biegun, M.; Mijowska, E., Superior synergy of g-C_3N_4/Cd compounds and Al-MOF-derived nanoporous carbon for photocatalytic hydrogen evolution. *Applied Catalysis B: Environmental* **2019,** *257*, 117906.

12. Li, Q.; Xue, D.-X.; Zhang, Y.-F.; Zhang, Z.-H.; Gao, Z.; Bai, J., A dual-functional indium–organic framework towards organic pollutant decontamination via physically selective adsorption and chemical photodegradation. *Journal of Materials Chemistry A* **2017,** *5* (27), 14182-14189.

13. Qin, L.; Chen, H.-Z.; Lei, J.; Wang, Y.-Q.; Ye, T.-Q.; Zheng, H.-G., Photodegradation of Some Organic Dyes over Two Metal–Organic Frameworks with Especially High Efficiency for Safranine T. *Crystal Growth & Design* **2017,** *17* (3), 1293-1298.

14. Wu, P.; Liu, Y.; Li, Y.; Jiang, M.; Li, X.-l.; Shi, Y.; Wang, J., A cadmium(ii)-based metal–organic framework for selective trace detection of nitroaniline isomers and photocatalytic degradation of methylene blue in neutral aqueous solution. *Journal of Materials Chemistry A* **2016,** *4* (42), 16349-16355.

15. Zhao, H.; Chen, Y.; Peng, Q.; Wang, Q.; Zhao, G., Catalytic activity of MOF(2Fe/Co)/carbon aerogel for improving H_2O_2 and OH generation in solar photo–electro–Fenton process. *Applied Catalysis B: Environmental* **2017,** *203*, 127-137.

16. Araya, T.; Chen, C.-c.; Jia, M.-k.; Johnson, D.; Li, R.; Huang, Y.-p., Selective degradation of organic dyes by a resin modified Fe-based metal-organic framework under visible light irradiation. *Optical Materials* **2017,** *64*, 512-523.

17. Yang, C.; Wu, S.; Cheng, J.; Chen, Y., Indium-based metal-organic framework/graphite oxide composite as an efficient adsorbent in the adsorption of rhodamine B from aqueous solution. *Journal of Alloys and Compounds* **2016,** *687*, 804-812.

18. Zhu, G.; Li, X.; Wang, H.; Zhang, L., Microwave assisted synthesis of reduced graphene oxide incorporated MOF-derived ZnO composites for photocatalytic application. *Catalysis Communications* **2017,** *88*, 5-8.

19. Xie, L.; Yang, Z.; Xiong, W.; Zhou, Y.; Cao, J.; Peng, Y.; Li, X.; Zhou, C.; Xu, R.; Zhang, Y., Construction of MIL-53(Fe) metal-organic framework modified by silver phosphate nanoparticles as a novel Z-scheme photocatalyst: Visible-light photocatalytic performance and mechanism investigation. *Applied Surface Science* **2019,** *465*, 103-115.

20. Guo, T.; Wang, K.; Zhang, G.; Wu, X., A novel α-Fe_2O_3@g-C_3N_4 catalyst: Synthesis derived from Fe-based MOF and its superior photo-Fenton performance. *Applied Surface Science* **2019,** *469*, 331-339.

21. Ahmad, M.; Chen, S.; Ye, F.; Quan, X.; Afzal, S.; Yu, H.; Zhao, X., Efficient photo-Fenton activity in mesoporous MIL-100(Fe) decorated with ZnO nanosphere for pollutants degradation. *Applied Catalysis B: Environmental* **2019,** *245*, 428-438.

22. Sarkar, C.; Basu, J. K.; Samanta, A. N., Synthesis of MIL-53(Fe)/SiO$_2$ composite from LD slag as a novel photo-catalyst for methylene blue degradation. *Chemical Engineering Journal* **2019,** *377*, 119621.

23. Tang, L.; Lv, Z.-q.; Xue, Y.-c.; Xu, L.; Qiu, W.-h.; Zheng, C.-m.; Chen, W.-q.; Wu, M.-h., MIL-53(Fe) incorporated in the lamellar BiOBr: Promoting the visible-light catalytic capability on the degradation of rhodamine B and carbamazepine. *Chemical Engineering Journal* **2019,** *374*, 975-982.

24. Zhang, H.; Zhu, C.; Cao, J.; Tang, Q.; Li, M.; Kang, P.; Shi, C.; Ma, M., Ultrasonic-Assisted Synthesis of 2D α-Fe$_2$O$_3$@g-C$_3$N$_4$ Composite with Excellent Visible Light Photocatalytic Activity. *Catalysts* **2018,** *8* (10), 457.

25. He, J.; Zhang, Y.; Zhang, X.; Huang, Y., Highly efficient Fenton and enzyme-mimetic activities of NH$_2$-MIL-88B(Fe) metal organic framework for methylene blue degradation. *Scientific reports* **2018,** *8* (1), 5159.

26. Hu, B.; Sun, Q.; Zuo, C.; Pei, Y.; Yang, S.; Zheng, H.; Liu, F., A highly efficient porous rod-like Ce-doped ZnO photocatalyst for the degradation of dye contaminants in water. *Beilstein journal of nanotechnology* **2019,** *10*, 1157-1165.

27. Shen, W.; Mu, Y.; Xiao, T.; Ai, Z., Magnetic Fe$_3$O$_4$–FeB nanocomposites with promoted Cr(VI) removal performance. *Chemical Engineering Journal* **2016,** *285*, 57-68.

28. He, H.; Cao, J.; Guo, M.; Lin, H.; Zhang, J.; Chen, Y.; Chen, S., Distinctive ternary CdS/Ni$_2$P/g-C$_3$N$_4$ composite for overall water splitting: Ni$_2$P accelerating separation of photocarriers. *Applied Catalysis B: Environmental* **2019,** *249*, 246-256.

29. Zheng, J.; Zhang, L., Designing 3D magnetic peony flower-like cobalt oxides/g-C_3N_4 dual Z-scheme photocatalyst for remarkably enhanced sunlight driven photocatalytic redox activity. *Chemical Engineering Journal* **2019,** *369*, 947-956.

30. Ma, M.; Yang, Y.; Li, W.; Ma, Y.; Tong, Z.; Huang, W.; Chen, L.; Wu, G.; Wang, H.; Lyu, P., Synthesis of yolk-shell structure Fe_3O_4/P(MAA-MBAA)-PPy/Au/void/TiO_2 magnetic microspheres as visible light active photocatalyst for degradation of organic pollutants. *Journal of Alloys and Compounds* **2019,** *810*, 151807.